Cell polarity and adherens junction formation inhibit epithelial Fas cell death receptor signaling

Laurent Gagnoux-Palacios, Hala Awina, Stéphane Audebert, Aurélie Rossin, Magali Mondin, Franck Borgese, Carlota Planas-Botey, Amel Mettouchi, Jean-Paul Borg, Anne-Odile Hueber

JCB Journal of Cell Biology

REPORT

Cell polarity and adherens junction formation inhibit epithelial Fas cell death receptor signaling

Laurent Gagnoux-Palacios[1], Hala Awina[1], Stéphane Audebert[3], Aurélie Rossin[1], Magali Mondin[1], Franck Borgese[1], Carlota Planas-Botey[1], Amel Mettouchi[2], Jean-Paul Borg[3,4], and Anne-Odile Hueber[1]

Finely tuned regulation of epithelial cell death maintains tissue integrity and homeostasis. At the cellular level, life and death decisions are controlled by environmental stimuli such as the activation of death receptors. We show that cell polarity and adherens junction formation prevent proapoptotic signals emanating from the Fas death receptor. Fas is sequestered in E-cadherin actin-based adhesion structures that are less able to induce downstream apoptosis signaling. Using a proteomic-based approach, we find that the polarity molecule Dlg1 interacts with the C-terminal PDZ-binding site in Fas and that this interaction decreases formation of the death-inducing complex upon engagement with Fas ligand (FasL), thus acting as an additional cell death protection mechanism. We propose that E-cadherin and Dlg1 inhibit FasL-induced cell death by two complementary but partially independent mechanisms that help to maintain epithelial homeostasis by protecting normal polarized epithelia from apoptosis. When polarity is lost, the Fas–cadherin–Dlg1 antiapoptotic complex is disrupted, and FasL can promote the elimination of compromised nonpolarized cells.

Introduction

Programmed cell death by apoptosis is a physiological process that leads to the elimination of damaged or potentially harmful cells to maintain tissue homeostasis. As a consequence, evading apoptosis is an integral part of tumor development and resistance to therapy (Hanahan and Weinberg, 2011). Cytokines of the TNF receptor family including the Fas receptor (CD95; TNFRSF6) are among the best-characterized apoptosis inducers. The apoptotic signaling induced by Fas upon activation by its ligand (FasL; TNFSF6) depends on the recruitment to the receptor of adaptor proteins and caspases forming a death-inducing signaling complex (DISC). This complex triggers caspase activation, responsible for the proteolytic cleavage of a broad spectrum of cellular targets, leading ultimately to cell death (Kischkel et al., 1995). Beside this prodeath function, Fas activation can also promote alternative nondeath signaling pathways leading to cell survival, proliferation, motility, cancer growth, and metastasis, depending on the cellular context (Peter et al., 2007). Invalidation and mutations of the Fas/FasL system in animal models and in human pathologies mainly demonstrate that Fas regulates tissue homeostasis in the immune system through the induction of apoptosis (Ramaswamy et al., 2009). Nevertheless, previous work reports that Fas is expressed in almost all human tissues including many epithelia such as the intestine (Chen et al., 2010). Therefore activation of Fas in these tissues has to be strictly controlled in order to maintain an equilibrium between survival and cell death signals.

At a cellular level, the life-and-death decision is controlled by different environmental cues including cell anchorage, which guarantees both cell–ECM adhesion and cell–cell adhesion thanks to different sets of specialized macrocomplexes. Both types of adhesion complexes have been shown to protect from cell death, but the exact mechanisms underlying these observations are still debated (Grossmann, 2002; Stupack and Cheresh, 2002). Cell–cell contacts are mediated by specialized cell surface receptors including E-cadherin, the main cell–cell adhesion molecule expressed in epithelial tissues. The cytosolic domain of E-cadherin interacts with catenins (α-, β-, and p-120), which are adaptor molecules that connect the receptor to the actin cytoskeleton to form intercellular adhesion complexes called adherens junctions (AJs; Niessen et al., 2011). AJs play a master organizer role in the establishment of apical–basal polarity and are found functionally associated with the Scrib–Dlg1–Hugl1 polarity complex (Reuver

[1]Université Côte d'Azur, Centre National de la Recherche Scientifique, Inserm, Institute de Biologie Valrose, Nice, France; [2]Institut Pasteur, Département de Microbiologie, Unité des Toxines Bactériennes, Université Paris Descartes, Paris, France; [3]Aix Marseille Université, Centre National de la Recherche Scientifique, Inserm, Institut Paoli-Calmettes, Centre de Recherche en Cancérologie de Marseille, Marseille Proteomics, Marseille, France; [4]Centre de Recherche en Cancérologie de Marseille, Cell Polarity, Cell Signaling, and Cancer, Equipe Labellisée Ligue Contre le Cancer, Aix Marseille Université, Centre National de la Recherche Scientifique, Inserm, Institut Paoli-Calmettes, Marseille, France.

Correspondence to Laurent Gagnoux-Palacios: gagnoux@unice.fr; Anne-Odile Hueber: hueber@unice.fr.

https://doi.org/10.1083/jcb.201805071

and Garner, 1998; Qin et al., 2005). In addition, AJs act as signaling platforms and are directly involved in the control of various pathways (Kobielak and Fuchs, 2006; McCrea et al., 2015). Their signaling capacities are at least in part due to their ability to associate with some cell surface receptors and to modulate their activities (Qian et al., 2004; Curto et al., 2007; Fukuhara et al., 2008; Lu et al., 2014). Alteration of AJs in epithelia is associated with loss of cell–cell contacts and cell polarity, which leads to uncontrolled proliferation and carcinoma formation (Jeanes et al., 2008; Stairs et al., 2011). However, loss of AJs in various animal models or in in vitro studies has been also associated with increased cell death (Carmeliet et al., 1999; Hofmann et al., 2007; Schneider et al., 2010), which is in agreement with a role of cell–cell junctions in the regulation of cell survival.

The possible role of cell–cell contacts and cell polarity in the control of Fas signaling has been largely unexplored. In this study, we report that E-cadherin plays a critical role in the regulation of Fas cell death signaling. Indeed, we demonstrate that in polarized colon epithelial cells, Fas is sequestered in E-cadherin actin-based adhesion structures, preventing its cell death signaling function. Moreover, we identify that the C-terminal PDZ domain of Fas interacts with the polarity molecule Dlg1, which accumulates together with AJs at cell–cell junctions. The interaction of Dlg1 with Fas inhibits Fas cell death signaling by impairing efficient formation of the DISC. Therefore, our findings uncover an important mechanistic link between cell–cell contacts and cell polarity along with the protection of polarized cohesive epithelial tissues from the Fas-induced death signal.

Results and discussion

Cell–cell contacts protect epithelial colon cells from FasL-induced cell death

To evaluate the importance of human epithelial tissue organization, and in particular cell–cell junctions, in the regulation of Fas proapoptotic signaling, we first analyzed the FasL-induced sensitivity of HCT15 cells, a human epithelial cell line of colon origin, which forms extensive cell–cell junctions and grows as independent islets (Fig. 1 A). Using time-lapse video microscopy experiments, we showed that induction of cell death by addition of FasL in HCT15 cells occurs preferentially in the cells located in the islet periphery that do not form mature junctions or in cells that do not form a cohesive islet (Fig. 1 A and Video 1). In contrast, cells that form extensive cell–cell junctions (i.e., located in the center of the islet) are protected from cell death. Treatment of HCT15 with staurosporine, a widely used chemical promotor of intracellular stress apoptosis, did not reveal a protective effect of cell–cell junctions (Fig. 1 A and Video 2), suggesting that cell–cell contacts specifically affect Fas signaling rather than having a general antiapoptotic effect. To rule out the possibility that the cell death resistance of cells located in the center of the islet was due to a limited diffusion of FasL through tight junction assembly, HCT15 cells were grown on permeable culture inserts. Video microscopy experiments showed that FasL treatment in both apical and basal reservoirs did not sensitize the central cells of the islet to FasL, demonstrating that this protective effect cannot be explained by a restriction of FasL diffusion at the basal side of the cells (Video 3).

Since maturation of cell–cell contacts including tight junctions and AJs requires the presence of extracellular calcium (Takeichi, 1988), we then analyzed the FasL-mediated cell death induction in HCT15 cells in which cell junctions were disrupted by growing cells in low-calcium conditions (Fig. 1 A and Video 4). Depletion of calcium resulted in a strong increase of FasL-induced cell death (Fig. 1, B–D and I), confirming the protective effect of cell–cell contacts in the regulation of Fas proapoptotic signaling.

To further characterize the nature of the cell–cell adhesion complex involved in the regulation of Fas signaling, we evaluated the role of AJs, the major cell–cell contact organizers (Halbleib and Nelson, 2006; Niessen et al., 2011), by specifically targeting their assembly. This was achieved by the transfection of HCT15 cells with siRNAs directed against either α-catenin, which is essential to nucleate mature AJs (Vasioukhin et al., 2001), or E-cadherin. We showed that the partial knockdown of AJ components alters cell–cell contact formation and results in a strong increase in the number of cells sensitive to FasL-mediated cell death (Fig. 1, E–H and J). Altogether, these experiments suggest that the formation of AJs in human epithelial cells inhibits the proapoptotic function of the Fas receptor.

Fas associates and forms a stable complex with AJs

Since the formation of AJs regulates Fas cell death signaling, we analyzed the localization of Fas at the border and the center of the cell islets. We found that at cell–cell contacts of confluent cells, Fas strongly colocalizes with E-cadherin (Fig. 2, A–C) and α-catenin (Fig. 2 F; Pearson coefficient of 0.815 and 0.655 for E-cadherin and α-catenin, respectively). Fas colocalized with E-cadherin together with actin in the zona adherens located at the apical end of lateral cell–cell contacts (Fig. 2, A and B, arrows) but also in cell contacts formed along the lateral surface of HCT15 epithelial cells (Fig. 2 B, arrowheads). Interestingly, Fas was less enriched in AJs in cells located at the periphery of the islet (Fig. 2, A and D), suggesting that maturation of cell–cell contacts favors Fas–E-cadherin association. Using proximity ligation assays (PLAs), we confirmed the molecular proximity of Fas and AJ components in HCT15 cells (Fig. 2 E). A similar colocalization of Fas and AJs was observed in human colon epithelial tissues, showing that Fas undergoes a similar polarized expression in vivo (Fig. 2 G).

To finely evaluate the role of AJs in the polarized expression of the Fas receptor, its localization was analyzed by immunofluorescence (IF) in HCT15, in which cell–cell contacts were disrupted by inhibiting α-catenin expression with siRNA. As shown in Fig. 2 F, in the absence of cell–cell junctions, Fas is no longer limited to a specific domain of the plasma membrane but rather becomes expressed all over the plasma membrane.

The formation of mature AJs corresponds with the assembly of cadherins and various cytoplasmic molecules together with the actin cytoskeleton into a macromolecular complex characterized by its detergent insolubility (Kinch et al., 1995). Since Fas associates with AJs in confluent cells, we analyzed whether the detergent solubility of Fas was dependent on AJ formation. Detergent solubility assays demonstrated that the proportion of Fas molecules associated with the detergent-insoluble cytoskeletal fraction decreased in HCT15 cells transfected with either α-catenin or E-cadherin siRNAs compared with cells transfected

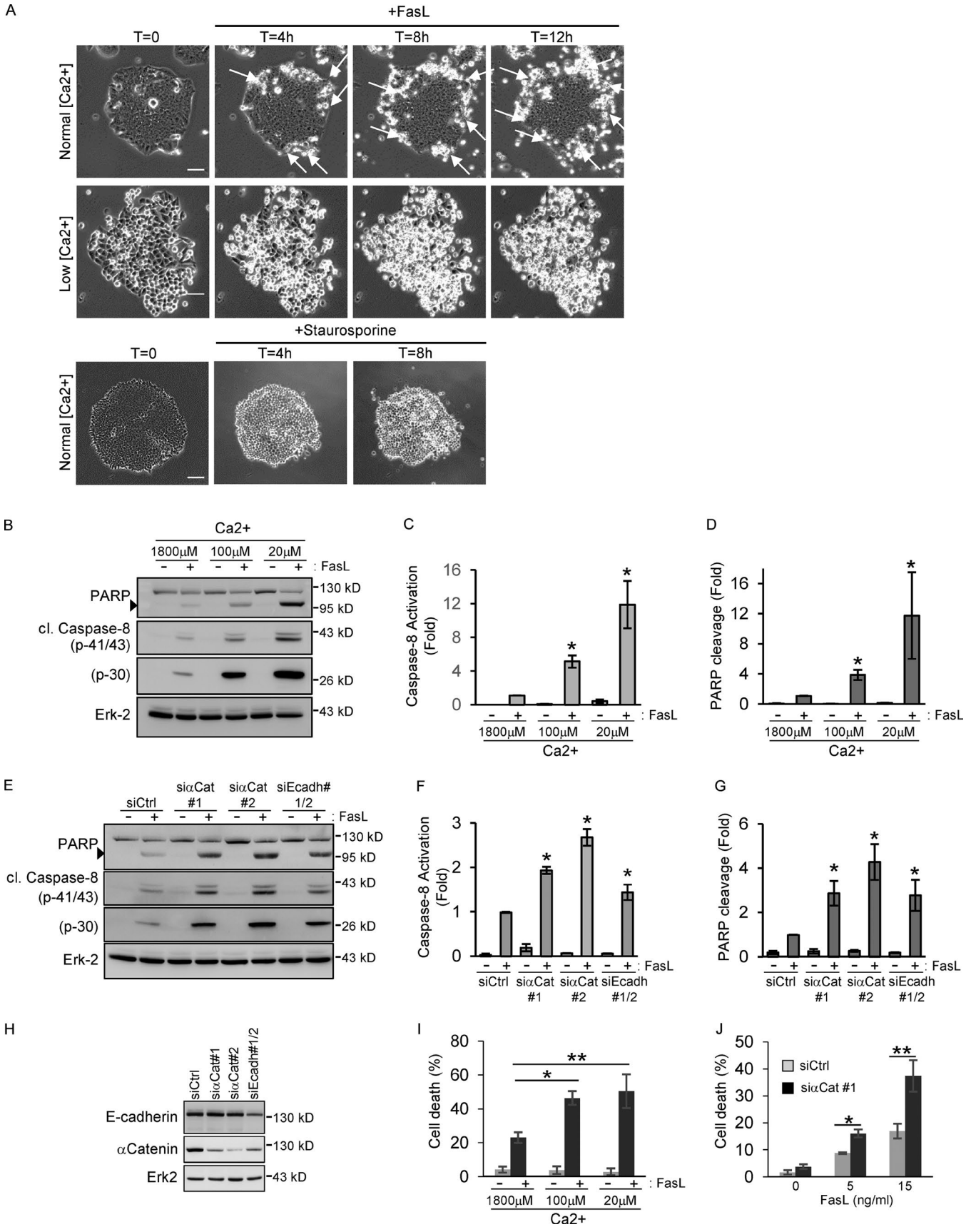

Figure 1. **AJs protect epithelial colon cells from FasL-induced cell death. (A)** HCT15 cells were grown in normal media or in low-calcium conditions (20 µM) before FasL (20 ng/ml + M2) or staurosporine (20 µM) treatment. Cell death was analyzed by phase-contrast time-lapse microscopy. Arrows indicate the localization of dead cells. Bar, 50 µm. **(B–D)** HCT15 cells were grown in media containing various concentrations of calcium (from 1,800 µM [normal

with a control siRNA (Fig. 2, H and I). Altogether, our data suggest that maturation of AJs controls the presence of Fas at sites of cell–cell contacts and its molecular association with this adhesion complex.

Sequestration of Fas in AJs inhibits FasL binding to the plasma membrane and consequently cell death signaling

To determine whether the inhibition of FasL-mediated cell death signaling found in confluent cells was due to a less-efficient binding of FasL to the cell surface, we developed a FasL-binding assay using FasL-coated beads. FasL-coated beads and noncoated beads were added to HCT15 cells forming mature cell–cell contacts or in which AJs were disrupted by transfecting cells with an α-catenin siRNA. Following 30 min incubation, FasL binding efficiency was determined using microscopic observations, bead counting, and IF studies (Fig. 3, A–E).

We showed that FasL-coated beads bound efficiently to HCT15 cells compared with noncoated control beads (Fig. 3 B). Moreover, IF studies followed by quantitative analyses revealed that FasL-coated beads induced a progressive accumulation of Fas and caspase-8 to small patches located beneath the area of bead–cell contacts (Fig. 3, C–E). As expected, a longer activation time (90 min) led to a strong cytosolic accumulation of activated caspase-8 associated with cell shrinkage (Fig. 3 C). Fas and caspase-8 recruitments were mostly observed beneath the beads attached to cells located at the border of the islet, suggesting that the efficiency of FasL binding is improved in bordering cells in which Fas does not accumulates in AJs. We next used the same FasL-coated bead assay to isolate Fas receptors together with DISC components. In agreement with our IF results, the quantity of Fas immunoprecipitated at each time point strongly increases during activation time, suggesting that the aggregation of Fas underneath each bead is a dynamic process (Fig. 3 F). These results demonstrated that FasL-coated beads preferentially bind to epithelial cells located at the margin of the islet, which do not form extensive cell–cell junctions.

We then compared the FasL-coated bead-binding efficiency and the caspase activation of HCT15 cells in which AJs were disrupted by knocking down α-catenin expression using specific siRNA. In the absence of AJs, FasL-coated beads were able to bind efficiently to the cells within the islet independently of their position and not only to the cells located at the periphery (Fig. 3 A), suggesting that the absence of AJs sensitizes cells within the islet to FasL binding. Counting the beads bound in each culture condition confirmed that the absence of AJs strikingly increased the binding efficiency of FasL-coated beads compared with control cells (siCtrl; Fig. 3 B). In agreement with these observations, more DISC components (Fas, caspase-8, and FADD) were pulled down by FasL-coated beads in α-catenin–knockdown cells compared with control cells (Fig. 3, F and G). Altogether, our results demonstrate that the disruption of AJs increases the availability of the Fas receptor for ligand binding, which strongly increases epithelial cell sensitivity to FasL-induced cell death.

The Fas C-terminal PDZ binding site interacts with various PDZ proteins and is required to stabilize and localize Fas at cell–cell contact

Recent examples demonstrate that PDZ domain–containing molecules interact directly with various cell surface receptors through a PDZ-binding site to target them to specific membrane domains including cell–cell contacts (Borg et al., 2000; Curto et al., 2007; Theisen et al., 2007; Chiasson-MacKenzie et al., 2015). Since Fas has been reported to contain a PDZ C-terminal binding motif (Yanagisawa et al., 1997), we tested the possibility that this domain was involved in the subcellular localization of Fas at cell–cell contacts. We generated HCT15 cells stably expressing a GFP-tagged version of the WT or a mutant form of Fas in which the last three amino acids (SLV), which compose a class I PDZ-binding motif (FasGFPΔSLV), were deleted (Fig. 4 A). Confocal analysis of the subcellular distribution of the FasGFPWT and FasGFPΔSLV ectopic receptors was performed on HCT15 cells stably expressing these constructs and forming extensive cell–cell junctions. This experiment showed that whereas FasGFP WT mainly colocalizes with E-cadherin at the lateral cell–cell junctions, FasGFPΔSLV not only does not efficiently associate with cell–cell junctions but also displays a cytosolic localization (Fig. 4, B and C). Cell surface biotinylation assays confirmed that the FasGFPΔSLV mutant is significantly less expressed at the cell surface compared with the WT form of Fas (Fig. 4, D and E). Detergent solubility assays demonstrated that the FasGFPΔSLV mutant is more soluble than its WT counterpart (Fig. S1 A), which correlates with a reduced association of the Fas PDZ mutant to cell–cell junctions. Thus, these data suggest that the Fas C-terminal PDZ binding site is required to target and/or to sequester Fas at cell–cell junctions.

We then used a previously described proteomic approach (Belotti et al., 2013) to identify the Fas molecular partner(s) able to associate with the PDZ-binding site of Fas and possibly be involved in its subcellular localization. Two peptides corresponding respectively with the last 20 amino acids of WT Fas and a mutant form lacking the PDZ-binding motif (FasΔSLV; Fig. 4 A) were bound to agarose beads and used as baits to pull down Fas molecular partners from HCT15 cell extracts. Following pull-down experiments, proteomic analysis allowed us to identify 53 molecules that were significantly pulled down with the FasWT peptide but not with the Fas peptide lacking the PDZ-binding motif (Fig. 4 F and Table S1). Among these proteins, 19 are PDZ domain–containing proteins, which have been associated with

conditions] to 20 µM [low conditions]) before FasL treatment (15 ng/ml + M2), and cell death was measured by monitoring caspase-8 activation (presence of p43/41 and p30 cleaved fragments) and PARP cleavage by IB. Relative caspase-8 activation (p41/43) and PARP cleavage were measured by quantitative densitometry (n = 3). **(E–G)** Cell death was induced by FasL treatment (15 ng/ml + M2) in HCT15 cells transfected with the indicated siRNAs and analyzed by IB as above. IBs were quantified by densitometry (n = 3). **(H)** The efficiency of each siRNA was verified by IB. **(I and J)** Cell death was analyzed by sub-G1 quantification (PI incorporation) in HCT15 grown in low-calcium conditions or transfected by the indicated siRNAs. Arrowheads in B and E indicate the cleaved forms of PARP. In all graphs, error bars represent means ± SEM. *, P < 0.05; **, P < 0.01; Student's t test.

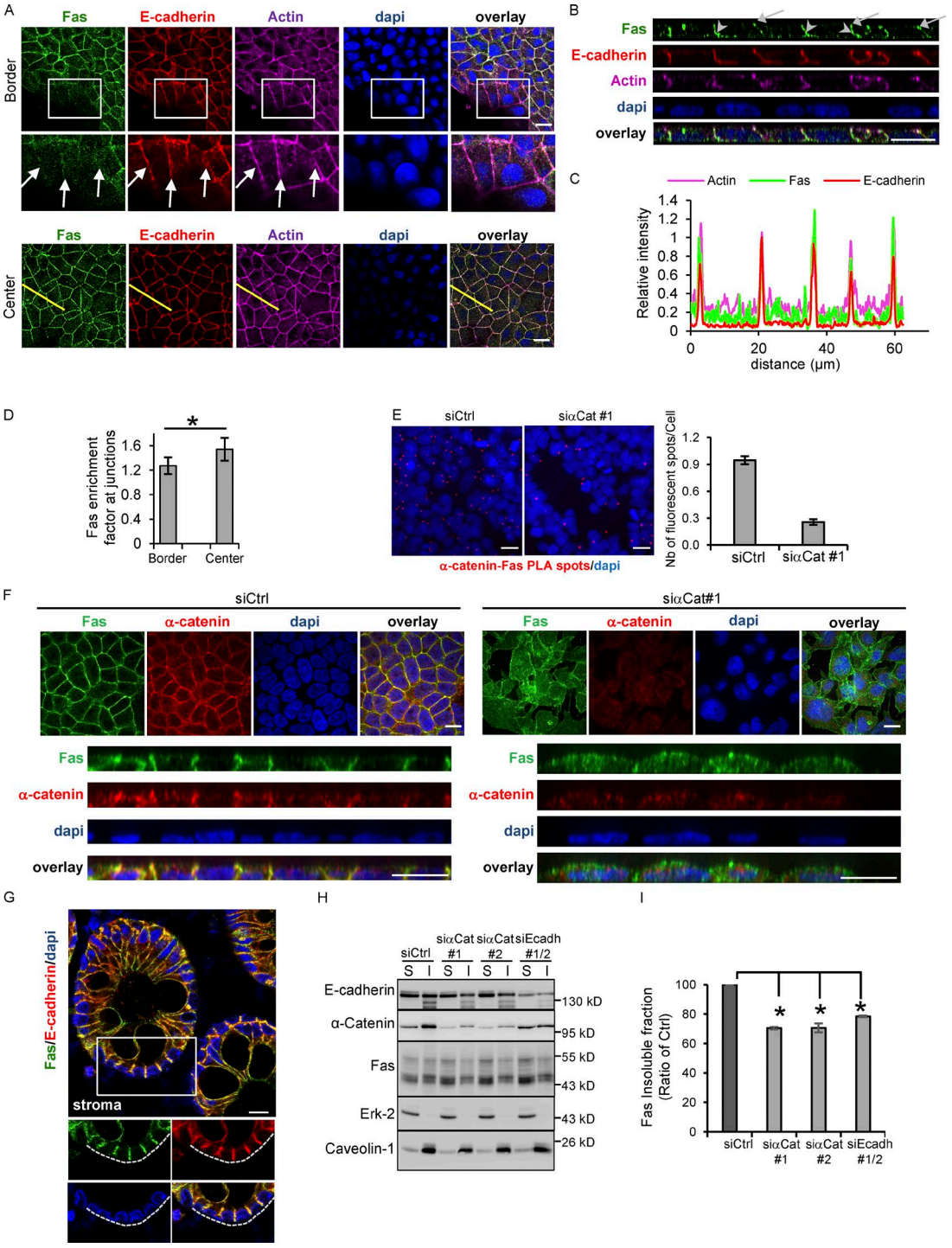

Figure 2. **Fas accumulates at cell–cell junctions and colocalizes with AJ components in both colorectal cell lines and colon tissue sections. (A)** Detection of E-cadherin, actin, and Fas by IF on HCT15 cells in border or center regions of the cell islet. An enlarged part of images from bordering cells is shown. Arrows indicate the diffuse localization of Fas at the plasma membrane in bordering cells. **(B)** XZ projection of Z stack acquired in A. Arrows and arrowheads indicate Fas–E-cadherin colocalization both at the zona adherens and along the lateral surface, respectively. **(C)** Line scan (yellow line in A) profile of fluorescence intensity of Fas, E-cadherin, and actin obtained at the center of the cell islet. **(D)** Quantification of the specific enrichment of Fas at cell–cell junctions in cells located at the center (confluent area) compared with the border of the HCT15 cell islets. Bars in graphs represent means ± SEM (n = 5). **(E)** PLA was used to determine the interaction of Fas and E-cadherin in HCT15 cells. Red fluorescent spots indicate colocalization of Fas and E-cadherin. PLA dots/cells in each condition were counted, and the right panel shows the mean of dots/cells ± SEM. One representative experiment is shown out of three. **(F)** Detection of Fas and α-catenin in HCT15 invalidated for α-catenin expression by using an siRNA approach. A XZ projection of Z stack is shown. **(G)** IF localization of Fas and E-cadherin in human colon tissue sections using confocal microscopy. **(H and I)** Fas detergent solubility in HCT15 cells transfected by the indicated siRNAs was analyzed by IB. S, soluble fraction; I, insoluble cytoskeletal fraction. Erk-2 and caveolin-1 were used as controls of soluble protein and membrane protein, respectively. Relative percentage of solubility of Fas in each condition was quantified by densitometry (n = 3). Bars in graphs represent means ± SEM (n = 5). Bars: 10 µM (A, B, E, and F); 20 µM (G). *, P < 0.05; Student's t test.

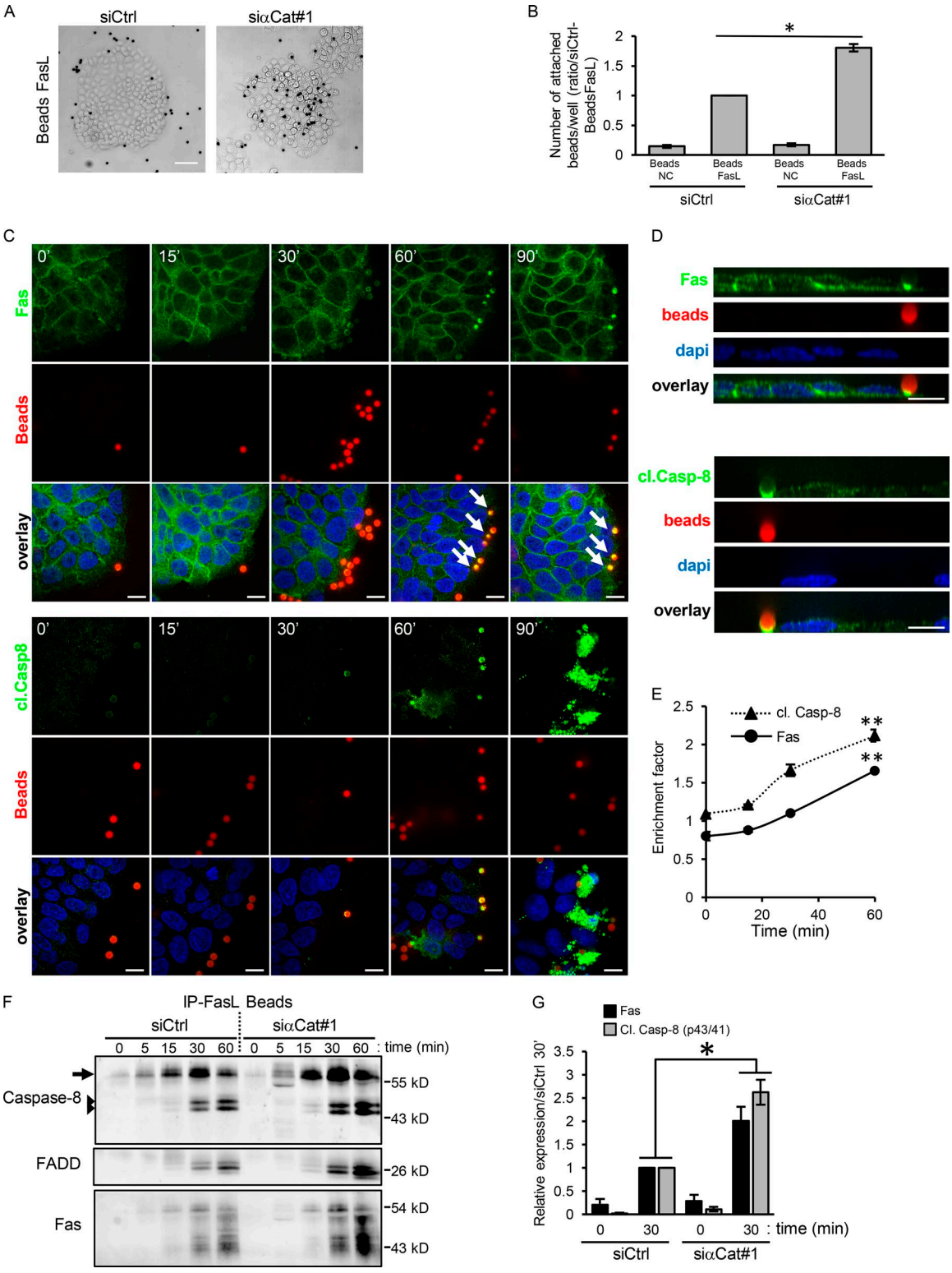

Figure 3. **AJs sequester Fas at site of cell–cell junction, and this impairs efficient FasL binding and therefore Fas cell death signaling. (A)** Binding assays of latex beads coated with FasL (Beads FasL) on HCT15 transfected with siRNAs against α-catenin and followed by phase-contrast microscopy. **(B)** FasL-coated or -noncoated (NC) beads attached to cells were counted using flow cytometry after cell lysis. Graphs represent means ± SEM (n = 3). **(C and D)** Detection of Fas and cleaved caspase-8 in HCT15 cells incubated with FasL-coated beads was done by IF at different time points. Beads appear in red (by autofluorescence). An XZ projection of the Z stack is shown. Arrows indicate the accumulation of Fas beneath the beads. **(E)** Accumulation of Fas and activated caspase-8 under FasL-coated beads was quantified. Graph represents mean ± SEM (n > 3). **(F)** FasL-coated beads were used to immunoprecipitate activated Fas from cell lysates of HCT15 cells transfected with indicated siRNAs. Fas, caspase-8, and FADD were detected by IB. Arrows and arrowheads indicate native caspase-8 and cleaved (activated) caspase-8, respectively. **(G)** Relative caspase-8 and Fas were quantified by densitometry at t = 0 or after 30 min FasL-coated bead activation (n = 3). Bars: 10 µM (C and D); 50 µM (A). *, P < 0.05; **, P < 0.01; Student's t test.

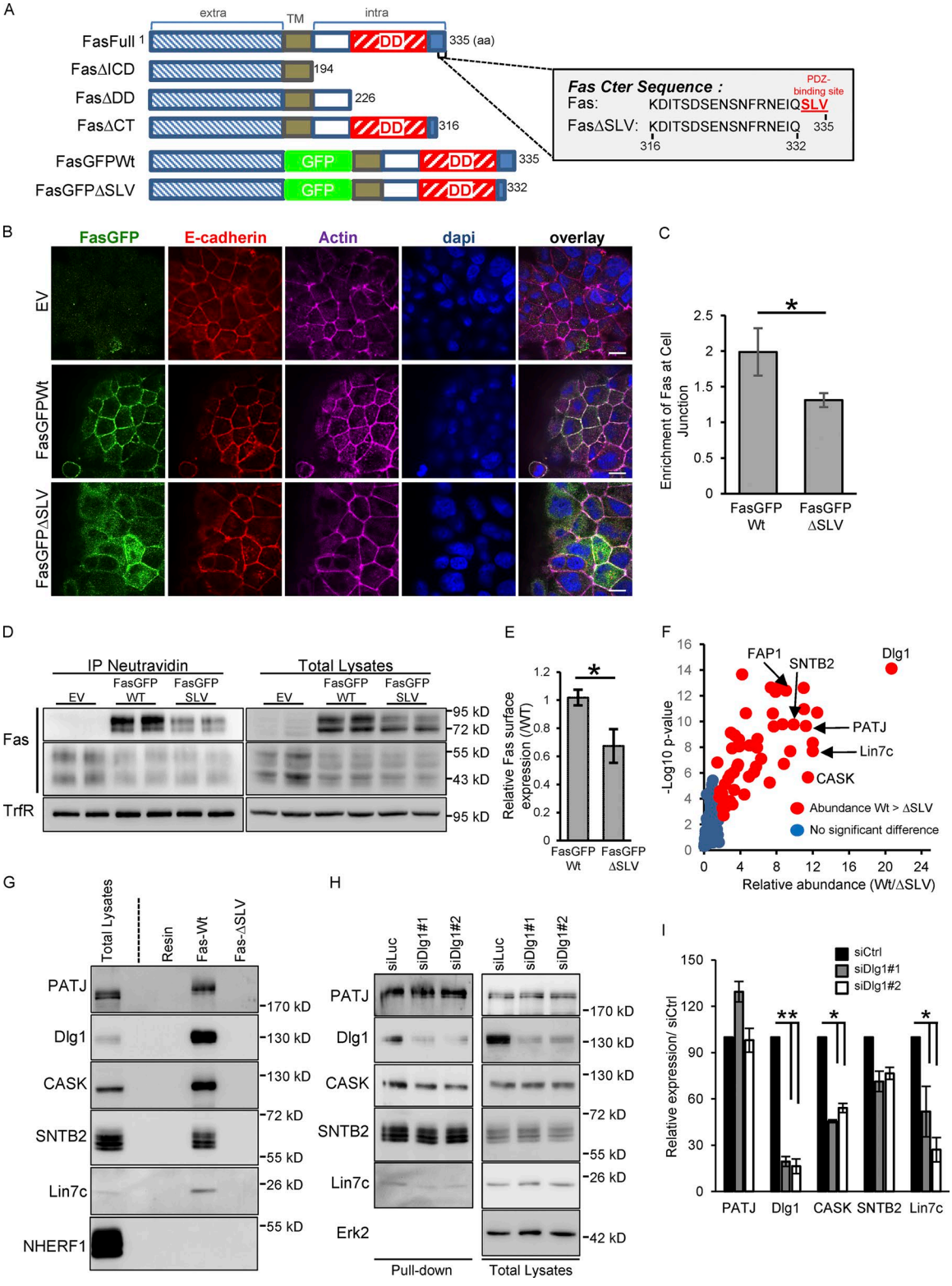

Figure 4. **Fas PDZ binding domain regulates Fas cell–cell junction localization and interacts with the polarity molecule Dlg1. (A)** Schematic representation of human Fas constructs and of the C-terminal sequence of Fas. The SLV C-terminal PDZ-binding motif is shown in red. TM, transmembrane domain. **(B)** Detection of E-cadherin and GFP by IF in HCT15 cells transduced with empty vector (EV), GFP-Fas WT, and ΔSLV mutant. **(C)** Quantification of the specific enrichment of GFP-Fas WT and ΔSLV mutant at cell–cell junctions. Error bars in graphs represent means ± SEM (n = 5). **(D)** Cell surface expression of GFP-Fas WT and ΔSLV mutant were compared using biotinylation assays. **(E)** Relative cell surface expression of GFP-Fas WT and of the ΔSLV mutant was quantified by densitometry. Error bars in graphs represent means ± SEM (n = 3). **(F)** Volcano plot summarizing comparison between the protein interacting with Fas C-terminal (Cter) peptide of WT and the ΔSLV mutant. The $\log_2$ ratio of protein intensities was plotted against negative $\log_{10}$ P values. Red circles correspond with proteins significantly more abundant in the WT than in the ΔSLV mutant ($P < 0.05$), and blue circles correspond with proteins without significant changes.

cell–cell junctions, cell polarity, receptor trafficking, and actin cytoskeleton interaction/regulation. FAP1 is the only protein already identified as a Fas interactor (Yanagisawa et al., 1997).

The most abundant protein found to interact with the Fas C-terminal part is the polarity molecule Dlg1. Dlg1 is a scaffold molecule containing four PDZ domains, and it belongs to the Scrib polarity complex. Dlg1 has been found to be tightly associated with AJs in various animal and cellular models (Reuver and Garner, 1998; Guo et al., 2014). Moreover, Dlg1 has been found to interact with several molecular partners also identified in our proteomic analysis such as CASK, Lin7c, and MPP7 (Fig. 4 F). Pulldown experiments followed by immunoblotting (IB) were used to verify the interaction of the Fas C-terminal domain with Dlg1 as well as with other abundant PDZ domain–containing proteins identified in our screen such as CASK, Lin7c, SNTB2, and PATJ but not with NHERF1, used as a negative control (Fig. 4 G). Using pulldown experiments, we also showed that the knockdown of Dlg1 expression by siRNAs affects the recruitment of several Fas molecular partners known to associate with Dlg1, such as CASK and Lin7c, but has only a minor effect on other PDZ-binding proteins (Fig. 4, H and I), supporting the idea that Dlg1 could organize a complex structural network composed of several proteins linked to the Fas C-terminal domain and connected to the actin cytoskeleton.

To further demonstrate the molecular interaction between Fas and Dlg1, Fas–Dlg1 association was verified by using both Fas immunoprecipitation (IP) experiments in 293T cells transiently transfected with Dlg1 and various Fas-deletion mutants (Fig. S1 B) as well as PLA on HCT15 cells (Fig. 5 D). Our results support the idea of a direct interaction between Fas and Dlg1 in epithelial cells.

The Dlg1 polarity molecule colocalizes with Fas and inhibits FasL-induced cell death signaling

As we mentioned, the Dlg1 polarity molecule has been found tightly associated with E-cadherin (Guo et al., 2014). As expected, IF experiments demonstrate that Dlg1 colocalizes with Fas at cell–cell junctions (Pearson's correlation coefficient of 0.73) in HCT15 cells, both at the border and in the center of the cell islets (Fig. 5, A and B).

We then investigated the importance of the Fas–Dlg1 association on Fas plasma membrane stability, localization, and signaling using a loss-of-function approach. IF experiments demonstrated that the knockdown of Dlg1 in HCT15 cells only slightly impacts Fas localization at the cell junctions (Fig. 5, A and C). In agreement with this result, solubilization assays revealed that siRNA silencing of Dlg1 in HCT15 has only a modest effect on Fas and α-catenin solubility (Fig. S2 A), suggesting that in HCT15 cells, AJ formation and Fas recruitment in AJs do not absolutely require Dlg1.

We then compared the binding efficiency of FasL-coated beads on HCT15 cells in which Dlg1 expression was knocked down by siRNAs. Dlg1 silencing in HCT15 did not statistically modify either the binding efficiency of FasL-coated beads or the preferential binding on peripheral cells observed in control cells (Figs. 3 A and S2 B). This suggests that the absence of Dlg1 is not sufficient to affect the Fas basal–lateral localization and to sensitize cells within islets to FasL binding as it occurs when cell–cell junctions are disrupted.

The potential role of Dlg1 in the modulation of Fas proapoptotic signaling was then studied by comparing FasL death sensitivity of HCT15 cells transfected with either control (siCtrl) or two different Dlg1 (siDlg1#1 and 2) siRNAs. The knockdown of Dlg1 significantly increased Fas-induced cell death as judged by IB using anti–cleaved caspase-8 and poly-ADP ribose polymerase (PARP) antibodies (Fig. 5, E and F). The increase of Fas cell death correlates with a slight increase of Fas total and cell surface expression in cells transfected by siRNAs against Dlg1 compared with a control receiving the control siRNA (siCtrl; Fig. S2 C). To analyze whether the role of Dlg1 in the regulation of Fas cell death signaling was dependent on AJ formation, we took advantage of another colorectal cell line named SW480 that does not form AJs due to a very low level of E-cadherin expression (Fig. S2 D; Conacci-Sorrell et al., 2003). The absence of Dlg1 in SW480 cells strongly increased FasL-induced cell death (Fig. 5, E and F) without significantly affecting Fas total or cell surface expression (Fig. S2 E).

Altogether, these data show that Dlg1 does not play an essential role in the sequestration of Fas in AJs but inhibits Fas cell death signaling by modulating the ability to optimally form a DISC upon FasL engagement. Since the Fas PDZ mutant is unable to efficiently localize in AJs, we hypothesize that other PDZ molecules may participate or compensate for the absence of Dlg1 to target/stabilize Fas at cell–cell junctions. Indeed, several PDZ proteins identified in our screen, such as MAGI-1/3, β2-syntrophin, MPP7, and CASK, have been found associated with cell–cell junctions. Further studies would be necessary to determine the exact mechanism by which Dlg1 interferes with cell death signaling. Indeed, several examples have shown that Dlg1 modulates receptor signaling by influencing their trafficking, localization, and molecular environment by recruiting adaptor molecules (Round et al., 2005; Fourie et al., 2014).

In this study, we uncover a new role of AJs as key regulators of Fas proapoptotic signaling in polarized epithelial cells. We clearly demonstrate that AJ formation is accompanied by the accumulation of Fas receptor within these adhesion complexes. This results in a strong inhibition of Fas-mediated cell death by impairing efficient FasL binding, thereby preventing the activation of the receptor. Moreover, we unravel that Fas accumulation in these lateral cellular domains requires the PDZ-binding domain of Fas. Using a proteomics approach, we reveal that this domain of Fas interacts preferentially with Dlg1, a scaffold molecule involved in the maintenance of cell polarity. We demonstrate that the Fas–Dlg1 interaction inhibits Fas cell death signaling,

(G) Pulldown experiment done with the C-terminal peptide of Fas (WT or FasΔSLV) followed by IB. **(H)** Pulldown experiment done with beads coupled to the C-terminal peptide of WT Fas on cell lysates of HCT15 transfected with the indicated siRNAs and followed by IB. **(I)** Relative expression of each protein pulldown with WT Fas C-terminal peptide was quantified by densitometry (n = 3). Bars, 10 µM. *, $P < 0.05$; Student's t test.

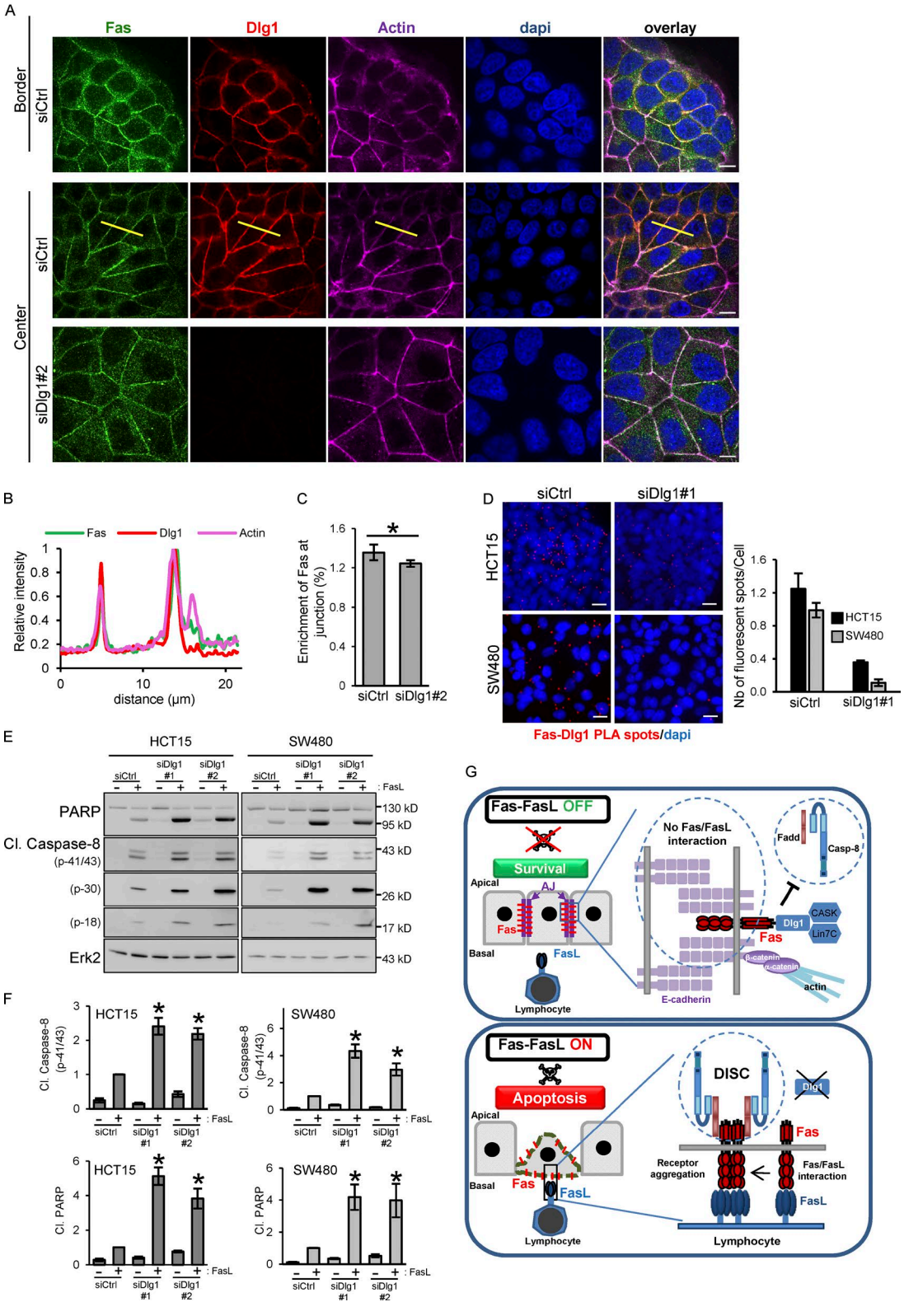

Figure 5. **Dlg1 is an inhibitor of Fas cell death signaling. (A)** Detection of Fas and Dlg1 by IF in control and Dlg1-knockdown HCT15 cells. **(B)** Line scan profile (yellow line in A) of fluorescence intensity of Fas, Dlg1, and actin in confluent cells. **(C)** Quantification of the specific enrichment of Fas at cell–cell junctions in control and Dlg1-knockdown HCT15 cells. Error bars in graphs represent means ± SEM (n = 5). **(D)** PLA was used to determine the interaction of Fas and Dlg1 in HCT15 cells as in Fig. 2 E. PLA dots/cells in each condition were counted, and the right panel shows the mean of dots/cells ± SEM. One representative experiment is shown (n = 3). **(E and F)** Cell death induced by FasL (15 ng/ml + M2) in HCT15 and SW480 cells transfected with the indicated siRNAs was analyzed as described above. Relative caspase-8 activation (p41/43) and PARP cleavage were quantified by densitometry (n = 3). **(G)** Schematic model summarizing the inhibitory function of E-cadherin and Dlg1 on Fas pro–cell death signaling. *, P < 0.05; Student's t test.

suggesting that Dlg1 interferes with the formation/stability of the death signaling complex. Therefore, accumulation of Fas at cell–cell junctions inhibits Fas cell death signaling by at least two different complementary mechanisms (Fig. 5 G).

Our study supports for the first time in human cells a molecular link between a scaffold protein involved in the maintenance of cell polarity and a cell death receptor. This result is in agreement with previous studies revealing the importance of cell polarity in the control of cell death (Weaver et al., 2002; Brumby and Richardson, 2003; Igaki et al., 2009; Frank et al., 2012). This cell death–regulatory mechanism is crucial to protect normal cells from apoptotic signals and to sense and eliminate abnormal cells from epithelial tissues in pathological conditions such as tumor development. Our data reveal a striking similarity with data obtained in *Drosophila melanogaster* in which activation of the fly TNF receptor Grnd by its ligand Eiger leads to the apoptotic elimination of mispolarized clonal epithelial cells due to siRNA silencing of Scrib or Dlg1 (Igaki et al., 2009; Andersen et al., 2015). Moreover, Gnrd is found associated with the Crumbs polarity complex and Veli (lin7), which regulates the fly TNF receptor signaling capacity. Our proteomics analysis demonstrates that Lin7c, the mammalian homologue of Veli, also interacts with Fas and that its association with Fas is dependent on Dlg1, suggesting that the control of TNF receptor signaling by polarity molecules has been conserved during evolution.

Finally, since Fas activation also leads to nonapoptotic signaling, in particular in the context of tumor development (Peter et al., 2007), it is possible that recruitment of Dlg1 and/or E-cadherin by Fas blocks cell death signaling while alternatively promoting nondeath pathways. Therefore, our study opens the door for further investigations to unravel the molecular mechanisms underlying the versatile regulation of Fas signaling by the cadherin–Dlg1 complex.

Materials and methods

Reagents and antibodies

For IB or IF, antibodies against anti-Fas (B10), Dlg1/SAP97 (2D11 and S19), Erk-2, Lin7 (C15), and CASK (H107) were purchased from Santa Cruz Biotechnology; anti–caspase-8 and Fadd were from MBL; anti–cleaved caspase-8 (cl. caspase-8) and PARP were from Cell Signaling Technology; anti–caspase-10 was from BioVision; anti–β-catenin, N-cadherin, and NHERF1 were from BD; anti-HA was from Covance; anti–E-cadherin was from Invitrogen; anti-Fas (EPR5700), p120, E-cadherin, and α-catenin were from Epitomics; anti-GAPDH was from EMD Millipore; anti-PATJ was from GeneTex; and anti–β2-syntrophin (SNTB2) was from Thermo Fisher Scientific. Fluorescent and HRP-conjugated secondary antibodies were from Molecular Probes and Jackson ImmunoResearch Laboratories, respectively, and staurosporine was from Sigma-Aldrich. For FasL treatment, Flag-recombinant human FasL from Alexis was cross-linked with anti-Flag M2 from Sigma-Aldrich.

Constructs

Human Fas ΔCter (pCR3.hFasDelCter) constructs were obtained using the QuikChange site-directed mutagenesis kit (Invitrogen) with pCR3-hFas as template and using 5′-CAGACTATCATCCTC TAGGACATTACTAGTGACTCAG-3′ and 5′-CTGAGTCACTAGTAA TGTCCTAGAGGATGATAGTCTG-3′ oligonucleotides, and they corresponded with the deletion of the last 20 aa of human Fas. pCR3-hFas, pCR3-hFasΔICD, and pCR3-hFasΔDD were kind gifts from P. Schneider (University of Lausanne, Epalinges, Switzerland) and correspond respectively with Fas full-length cDNA (FasFull), deleted of the entire cytoplasmic domain (FasΔICD), and deleted of the C-terminal domain of Fas including the death domain (DD; FasΔDD). Fas GFP WT was a kind gift from J. Lane (University of Bristol, Bristol, UK). Fas GFP ΔSLV was obtained by deleting the SLV tripeptide by PCR. Both GFP constructs (WT and mutant) were cloned in the retroviral vector LXSN. Rat Dlg1-expressing vector was a gift from L. Banks (International Centre for Genetic Engineering and Biotechnology, Trieste, Italy).

Cell Culture, treatment, transfection, and viral infection

All cell lines were grown in DMEM supplemented with 10% FBS supplemented with nonessential amino acids (Gibco; Thermo Fischer Scientific). Transient transfection of plasmids in 293T was obtained by using the JetPRIME transfection reagent (Polyplus). For siRNA transfection, cells were transiently transfected using RNAiMAX lipofectamine reagent (Invitrogen) according to the manufacturer's procedure. α-Catenin, E-cadherin, and Dlg1 silencing were obtained using individual sequences: for α-catenin #1, 5′-GAAGAGAGGUCGUUCUAAG-3′; and #2, 5′-GAU GGUAUCUUGAAGUUGA-3′; and for Dlg1 #1, 5′-CCAUAGAAC GGGUUAUUAA-3′; and #2, 5′-GGAAGACAUUUACAACCAAGU-3′. E-cadherin silencing was obtained using a mix of two individual siRNAs (#1, 5′-GGCCUGAAGUGACUCGUAA-3′; #2, 5′-GGGACA ACGUUUAUUACUA-3′), and siRNA targeting luciferase was used as control (siCtrl, 5′-CGUACGCGGAAUACUUCGA-3′).

Infection of HCT15 with LXSN retroviral vector expressing Fas GFP WT and mutant was performed as described (Gagnoux-Palacios et al., 2005). Briefly, infectious supernatants generated using phoenix retroviral producer cell line supplemented with polybrene were added to actively growing cells at high MOI followed by spinoculation procedure. Expressing cells were selected for neoresistance to geneticin (500 µg/ml; Sigma-Aldrich) 48 h after infection.

Preparation of FasL-coated beads

400 µl magnetic beads linked to human anti-mouse IgG (Dynabeads; Invitrogen) were incubated with 40 µg M2 antibody for 1 h at RT in DMEM and 0.1% BSA on a wheel. M2-coated beads were washed and incubated one more hour with 2 µg recombinant FasL in the same conditions. After washing, beads were kept at 4°C in sterile conditions or used immediately for Fas activation. The same amount of uncoated beads was used as a control in these experiments.

Cell death assays

For cell death experiments, cells were incubated with indicated doses of recombinant human Flag-FasL (FasL) cross-linked with 1 µg/ml M2 antibody or with FasL-coated beads. After the indicated incubation time at 37°C and 5% CO_2, cells were collected and fixed in ice-cold 70% ethanol. Cells were washed in 38 mM sodium citrate, pH 7.4, stained for 20 min at 37°C with 50 µg/ml propidium

iodide (PI; Sigma-Aldrich) and 5 µg/ml RNaseA (Sigma-Aldrich) in 38 mM sodium citrate, and analyzed by flow cytometry using the Fortessa analyzer (BD). The proportion of apoptotic cells as represented by the sub-G1 peak was determined. Alternatively, cell death induced by FasL/M2 cotreatment or staurosporine (20 µM) was analyzed by video microscopy using an inverted ZEISS Axiovert200 microscope equipped with a Zeiss 10× Plan-Neofluar PH1 dry 0.3 NA objective lens. Images were acquired with a monochrome Neo sCMOS camera (Andor Technology) controlled with MetaMorph 7.7 software (Molecular Devices).

IF and FasL-binding assay

For immunolabeling, cells attached to glass coverslips were fixed with 3.7% formaldehyde for 15 min at RT and either subsequently permeabilized with 0.1% Triton X-100 or incubated on ice in cold methanol for 5 min. After 1-h saturation in PBS containing 1% BSA and overnight incubation at 4°C with the indicated primary antibodies, cells were washed with PBS and incubated with fluorescent-conjugated secondary antibodies (Molecular Probes/Invitrogen) and DAPI (Sigma-Aldrich). Samples were analyzed using an inverted IX81 Olympus microscope (Olympus) equipped with a motorized XY stage (Prior Scientific), a CSU-X1 confocal head (Yokogawa Electric Corporation), and a sensitive iXon DU-897-BV electron-multiplying charge-coupled device (EMCCD) camera (Andor Technology). Z stacks were acquired using a piezo stage NanoScan Z100 (Prior Scientific). The system was controlled using MetaMorph software. Fresh frozen sections of human colon were immunolabeled using a similar procedure and analyzed on an LSM780 confocal microscope (Zeiss) using a 40× 1.1 NA water objective. All experimental and control images of the IF or phase-contrast data were collected using identical imaging settings, and images were merged using Fiji software tools (ImageJ; National Institutes of Health; Schindelin et al., 2012). For FasL-binding assay, cells were incubated with FasL-coated beads or uncoated beads (as a control) in DMEM and 0.1% BSA for 30 min at 37°C and 5% CO_2. After extensive washing to remove unbound beads, cells were fixed with a solution of 3.7% formaldehyde in PBS, and phase-contrast pictures of each well were performed using a 10× objective. Alternatively, cells were lysed, and lysates were subjected to flow cytometry using the HTS Plate Manager (BD) to calculate the number of cell-fixed beads in each condition.

Specific enrichment quantification

Fas specific enrichment at cell–cell junctions or Fas and caspase recruitment at FasL-coated beads were quantified using the same the process with Fiji software. Briefly, reference regions, either cell–cell junctions (labeled by E-cadherin, actin, and Dlg1) or bead contours were defined using intensity-based thresholds. The intensity of the marker of interest, endogenous Fas, FasGFP, or cleaved caspase-8, was measured inside those predefined contours (cell–cell junctions or beads). Then, the intensity of the marker of interest, endogenous Fas, FasGFP, or cleaved caspase-8, was measured outside those predefined contours to measure the basal level of expression. Finally, the enrichment factor was calculated by the ratio of the signal of interest inside/outside of the junctions or beads. An enrichment factor value >1 meant that the protein of interest was specifically enriched either in the cell–cell junction or at the FasL-coated beads.

DuoLink in situ PLA

To detect the interaction between Fas and Dlg1 or α-catenin, we used the DuoLink in situ PLA (Olink Bioscience) according to the manufacturer's protocol. HCT15 or SW480 cells were seeded on poly-L-lysine (40 µg/ml)–coated microscope slides. Cells were fixed with 4% PFA and permeabilized with 0.5% Triton X-100. Cells were immunolabeled with primary antibodies: anti-Fas, anti-Dlg1, or anti–α-catenin overnight at 8°C. The secondary antibodies (PLA probes supplied in the DuoLink kit) were incubated for 1 h at 37°C. Images were collected on an inverted AxioObserver Z1 microscope (Zeiss) equipped with a 63× 1.4 NA Plan Apochromat DICIII oil objective lens. Images were acquired with a monochrome EMCCD iXON+897 camera (Andor Technology) controlled with MetaMorph 7.8 software. A fluorescence signal indicated that two proteins were separated by <40 nm. PLA dots and nuclei were calculated in each field, and results were expressed as the mean number of count/cells.

Peptide pulldown, IP, and IB

Peptides corresponding with carboxyl terminals of human Fas (316–335 aa [Fas] or 316–332 aa [FasΔSLV]) were synthesized (GenScript) and cross-linked to NHS-activated Sepharose 4 Fast Flow beads according to the manufacturer's instructions (GE Healthcare). Pulldown experiments were performed using HCT15 cell lysates, and interacting proteins were identified by IB. Briefly, peptide-coated beads were added to cell lysates and incubated for 2 h at 4°C. Beads were washed in lysis buffer (20 mM Hepes, pH 7.5, 150 mM NaCl, 0.2 mM EDTA, 0.5% Triton X-100, 2 mM $MgCl_2$, 2 mM DTT, 10 mM NaF, 20 mM β-glycerophosphate, and a mix of protease inhibitors), and proteins bound to beads were separated by SDS-PAGE classical procedure. For IP, 293 cells transfected with Fas and rat Dlg1-encoding plasmids were lysed at 4°C in IP buffer: 20 mM Hepes, pH 7.5, 150 mM NaCl, 0.2 mM EDTA, 0.5% Triton X-100, 10% glycerol, 2 mM $MgCl_2$, 10 mM NaF, 20 mM β-glycerophosphate, and a mix of protease inhibitors. The postnuclear supernatants obtained after centrifugation at 10,000 *g* for 10 min at 4°C were incubated with protein G Sepharose beads (Invitrogen) coupled to Fas antibody (Apo1.3) for 2 h. After washes with lysis buffer, beads were eluted with sample buffer at 95°C for 5 min and subjected to SDS-PAGE and IB. To analyze DISC formation, cells were incubated with 20 µl FasL-coated beads at 4°C for 30 min to allow bead deposition and initial attachment. Cell plates were lysed directly ($t = 0$) or transferred at 37°C for various periods of time (from 15 to 60 min) to trigger Fas activation and DISC formation before cell lysis in IP buffer. Cell lysates were sonicated, and protein concentration was evaluated. The same quantity of protein (1 mg) was used in the IP for each condition. Lysates were incubated for 1 h at 4°C under agitation. FasL-coated beads were then isolated using a magnet and washed four times with the lysis buffer. Magnetic beads were resuspended in Laemmli buffer, and protein extracts were separated by SDS-PAGE followed by classical IB procedures. IB analysis of total proteins was performed according to standard protocols. Briefly, cells were lysed in 50 mM Tris, pH 8, 150 mM NaCl, 2 mM EDTA, 1% NP-40, 0.5% deoxycholate,

and 0.1% SDS containing phosphatase and protease inhibitors. After preclearing by centrifugation and quantification, the solubilized denatured proteins were resolved by SDS-PAGE. IB was performed using the indicated primary antibody and HRP-coupled secondary antibody (Jackson ImmunoResearch Laboratories). Quantitative densitometry was performed using ImageJ.

Cell surface biotinylation

The presence of Fas at the cell surface was assessed by biotinylation assays followed by IP with agarose beads coupled with avidin according to the manufacturer's instructions. Briefly, cells were washed three times in PBS, pH 8, 1 mM $MgCl_2$, and 0.5 mM $CaCl_2$ at 4°C, and then sulfo-NHS-SS-biotin (Pierce) was added to a final concentration of 0.2 mg/ml for 30 min at 4°C. The monolayers were washed once in ice-cold PBS, pH 8, 1 mM $MgCl_2$, and 0.5 mM $CaCl_2$ and incubated with PBS solution containing 100 mM glycine for 10 min to block free biotin. After incubation, cells were washed once with ice-cold PBS and lysed in lysis buffer. The same amount of biotinylated proteins were precipitated with Neutravidin-conjugated agarose (Pierce) in each condition for 2 h. The beads were washed three times in lysis buffer for 5 min each and resuspended in Laemmli buffer. Protein extracts were separated by SDS-PAGE followed by classical IB procedures.

Mass spectroscopy analysis

Following peptide pulldown (see above), protein extracts were loaded and stacked on a NuPAGE gel (Life Technologies). Stained bands were submitted to an in-gel trypsin digestion. Peptide extracts were reconstituted with 0.1% trifluoracetic acid in 4% acetonitrile and analyzed by liquid chromatography (LC)–tandem mass spectrometry (MS/MS) using an Orbitrap Fusion Lumos Tribrid mass spectrometer (Thermo Fisher Scientific) online with an Ultimate 3000RSLCnano chromatography system (Thermo Fisher Scientific). Protein identification and quantification were processed using the MaxQuant computational proteomics platform (version 1.5.3.8) using the human subset of the SwissProt database (date 2018.01; 20,244 entries). The statistical analysis was done with Perseus program (version 1.5.6.0). Differential proteins were detected using a two-sample *t* test at 0.01 and 0.05 permutation-based false discovery rate. The mass spectrometry proteomics data, including search results, have been deposited in the ProteomeXchange Consortium via the PRIDE partner repository with the dataset identifier PXD009659.

Detergent solubility assay

The detergent solubility assay was derived from Gimond et al. (1999). Cell cultures were lysed 20 min on ice in 300 µl of 0.5% Brij58, 50 mM Tris, pH 7.4, 150 mM NaCl, 1 mM EDTA, 1 mM EGTA, 5 mM NaF, 20 mM β-glycerophosphate, and 10 mM sodium pyrophosphate in the presence of protease inhibitors, and cell lysates were centrifuged at 14,000 rpm for 10 min to obtain the soluble fraction of protein. The pellet represents the cytoskeleton-associated protein (insoluble fraction) and was resuspended in 400 µl Laemmli buffer. To compare the solubility of each protein, 1:15 soluble fraction (representing ∼20 µg soluble protein) and 1:5 insoluble protein (80 µl) for each condition were separated in SDS-PAGE followed by classical IB procedures. Quantitation of protein expression was performed using ImageJ and was used to determine the proportion of each protein in soluble versus insoluble fractions. The solubility index for each protein represents the ratio of total amount of soluble versus insoluble. One representative experiment was shown out of three.

Statistical analysis

Data were analyzed using a homoscedastic two-tailed *t* test. $P < 0.05$ was considered statistically significant. *, $P < 0.05$; **, $P < 0.005$.

Online supplemental material

Fig. S1 describes the role of the Fas C-terminal PDZ-binding site in the regulation of Fas detergent solubility and Fas-Dlg1 binding. Fig. S2 shows the impact of the Dlg1 polarity molecule on Fas detergent solubility, FasL binding, and both total and cell surface Fas expression. Video 1 shows the effects of FasL treatment on an islet of HCT15 cells. Video 2 shows the effects of the treatment of the same cell line by staurosporine, a common chemical inducer of apoptosis. Video 3 and 4 are filmed in similar conditions to Video 1 except that HCT15 cells were grown on a semipermeable cell culture or in culture media depleted of calcium, respectively. Table S1 shows the comprehensive listing of all Fas interactors identified by pulldown assay and LC-MS/MS analysis.

Acknowledgments

We are grateful to Lawrence Banks, Jon Lane, and Pascal Schneider for providing us with expression vectors (human rat Dlg1, human GFP-Fas, and human Fas, respectively), to the Institute de Biologie Valrose facilities (Histology–S. Rekima and Cytometry–A. loubat), and to Sébastien Huault for technical assistance.

This work was supported by institutional funding from Inserm, Centre National de la Recherche Scientifique, and by grants from the Association pour la Recherche sur le Cancer and the LABEX SIGNALIFE program (ANR-11-LABX-0028-01). J.-P. Borg's laboratory is supported by La Ligue Nationale Contre le Cancer (Label Ligue) and Ruban Rose Award. J.-P. Borg is a scholar of Institut Universitaire de France. Proteomic analyses were done using the mass spectrometry facility of Aix Marseille Université Proteomics labeled "Plateforme technologique de l'Université Aix-Marseille," supported by Infrastructures Biologie Santé et Agronomie, the Cancéropôle PACA, the Provence-Alpes-Côte d'Azur Region, the Institut Paoli-Calmettes, and the Centre de Recherche en Cancérologie de Marseille.

The authors declare no competing financial interests.

Author contributions: L. Gagnoux-Palacios and A.O. Hueber conceived the study and wrote the manuscript; L. Gagnoux-Palacios designed, performed, and analyzed most experiments; H. Awina, A. Rossin, C. Planas-Botey, and A. Mettouchi performed experiments; S. Audebert performed and analyzed MS/MS experiments; M. Mondin performed, analyzed, and quantified IF experiments; F. Borgese performed and analyzed PLA experiments; J.-P. Borg conceived and analyzed MS/MS experiments.

Submitted: 14 May 2018
Revised: 27 June 2018
Accepted: 24 August 2018

References

Andersen, D.S., J. Colombani, V. Palmerini, K. Chakrabandhu, E. Boone, M. Röthlisberger, J. Toggweiler, K. Basler, M. Mapelli, A.-O. Hueber, and P. Léopold. 2015. The Drosophila TNF receptor Grindelwald couples loss of cell polarity and neoplastic growth. *Nature.* 522:482–486. https://doi.org/10.1038/nature14298

Belotti, E., J. Polanowska, A.M. Daulat, S. Audebert, V. Thomé, J.C. Lissitzky, F. Lembo, K. Blibek, S. Omi, N. Lenfant, et al. 2013. The human PDZome: a gateway to PSD95-Disc large-zonula occludens (PDZ)-mediated functions. *Mol. Cell. Proteomics.* 12:2587–2603. https://doi.org/10.1074/mcp.O112.021022

Borg, J.P., S. Marchetto, A. Le Bivic, V. Ollendorff, F. Jaulin-Bastard, H. Saito, E. Fournier, J. Adélaïde, B. Margolis, and D. Birnbaum. 2000. ERBIN: a basolateral PDZ protein that interacts with the mammalian ERBB2/HER2 receptor. *Nat. Cell Biol.* 2:407–414. https://doi.org/10.1038/35017038

Brumby, A.M., and H.E. Richardson. 2003. scribble mutants cooperate with oncogenic Ras or Notch to cause neoplastic overgrowth in Drosophila. *EMBO J.* 22:5769–5779. https://doi.org/10.1093/emboj/cdg548

Carmeliet, P., M.G. Lampugnani, L. Moons, F. Breviario, V. Compernolle, F. Bono, G. Balconi, R. Spagnuolo, B. Oosthuyse, M. Dewerchin, et al. 1999. Targeted deficiency or cytosolic truncation of the VE-cadherin gene in mice impairs VEGF-mediated endothelial survival and angiogenesis. *Cell.* 98:147–157. https://doi.org/10.1016/S0092-8674(00)81010-7

Chen, L., S.M. Park, J.R. Turner, and M.E. Peter. 2010. Cell death in the colonic epithelium during inflammatory bowel diseases: CD95/Fas and beyond. *Inflamm. Bowel Dis.* 16:1071–1076. https://doi.org/10.1002/ibd.21191

Chiasson-MacKenzie, C., Z.S. Morris, Q. Baca, B. Morris, J.K. Coker, R. Mirchev, A.E. Jensen, T. Carey, S.L. Stott, D.E. Golan, and A.I. McClatchey. 2015. NF2/Merlin mediates contact-dependent inhibition of EGFR mobility and internalization via cortical actomyosin. *J. Cell Biol.* 211:391–405. https://doi.org/10.1083/jcb.201503081

Conacci-Sorrell, M., I. Simcha, T. Ben-Yedidia, J. Blechman, P. Savagner, and A. Ben-Ze'ev. 2003. Autoregulation of E-cadherin expression by cadherin-cadherin interactions. *J. Cell Biol.* 163:847–857. https://doi.org/10.1083/jcb.200308162

Curto, M., B.K. Cole, D. Lallemand, C.H. Liu, and A.I. McClatchey. 2007. Contact-dependent inhibition of EGFR signaling by Nf2/Merlin. *J. Cell Biol.* 177:893–903. https://doi.org/10.1083/jcb.200703010

Fourie, C., D. Li, and J.M. Montgomery. 2014. The anchoring protein SAP97 influences the trafficking and localisation of multiple membrane channels. *Biochim. Biophys. Acta.* 1838:589–594. https://doi.org/10.1016/j.bbamem.2013.03.015

Frank, S.R., J.H. Bell, M. Frödin, and S.H. Hansen. 2012. A βPIX-PAK2 complex confers protection against Scrib-dependent and cadherin-mediated apoptosis. *Curr. Biol.* 22:1747–1754. https://doi.org/10.1016/j.cub.2012.07.011

Fukuhara, S., K. Sako, T. Minami, K. Noda, H.Z. Kim, T. Kodama, M. Shibuya, N. Takakura, G.Y. Koh, and N. Mochizuki. 2008. Differential function of Tie2 at cell-cell contacts and cell-substratum contacts regulated by angiopoietin-1. *Nat. Cell Biol.* 10:513–526. https://doi.org/10.1038/ncb1714

Gagnoux-Palacios, L., C. Hervouet, F. Spirito, S. Roques, M. Mezzina, O. Danos, and G. Meneguzzi. 2005. Assessment of optimal transduction of primary human skin keratinocytes by viral vectors. *J. Gene Med.* 7:1178–1186. https://doi.org/10.1002/jgm.768

Gimond, C., A. van Der Flier, S. van Delft, C. Brakebusch, I. Kuikman, J.G. Collard, R. Fässler, and A. Sonnenberg. 1999. Induction of cell scattering by expression of beta1 integrins in beta1-deficient epithelial cells requires activation of members of the rho family of GTPases and downregulation of cadherin and catenin function. *J. Cell Biol.* 147:1325–1340. https://doi.org/10.1083/jcb.147.6.1325

Grossmann, J. 2002. Molecular mechanisms of "detachment-induced apoptosis--Anoikis". *Apoptosis.* 7:247–260. https://doi.org/10.1023/A:1015312119693

Guo, Z., L.J. Neilson, H. Zhong, P.S. Murray, S. Zanivan, and R. Zaidel-Bar. 2014. E-cadherin interactome complexity and robustness resolved by quantitative proteomics. *Sci. Signal.* 7:rs7. https://doi.org/10.1126/scisignal.2005473

Halbleib, J.M., and W.J. Nelson. 2006. Cadherins in development: cell adhesion, sorting, and tissue morphogenesis. *Genes Dev.* 20:3199–3214. https://doi.org/10.1101/gad.1486806

Hanahan, D., and R.A. Weinberg. 2011. Hallmarks of cancer: the next generation. *Cell.* 144:646–674. https://doi.org/10.1016/j.cell.2011.02.013

Hofmann, C., F. Obermeier, M. Artinger, M. Hausmann, W. Falk, J. Schoelmerich, G. Rogler, and J. Grossmann. 2007. Cell-cell contacts prevent anoikis in primary human colonic epithelial cells. *Gastroenterology.* 132:587–600. https://doi.org/10.1053/j.gastro.2006.11.017

Igaki, T., J.C. Pastor-Pareja, H. Aonuma, M. Miura, and T. Xu. 2009. Intrinsic tumor suppression and epithelial maintenance by endocytic activation of Eiger/TNF signaling in Drosophila. *Dev. Cell.* 16:458–465. https://doi.org/10.1016/j.devcel.2009.01.002

Jeanes, A., C.J. Gottardi, and A.S. Yap. 2008. Cadherins and cancer: how does cadherin dysfunction promote tumor progression? *Oncogene.* 27:6920–6929. https://doi.org/10.1038/onc.2008.343

Kinch, M.S., G.J. Clark, C.J. Der, and K. Burridge. 1995. Tyrosine phosphorylation regulates the adhesions of ras-transformed breast epithelia. *J. Cell Biol.* 130:461–471. https://doi.org/10.1083/jcb.130.2.461

Kischkel, F.C., S. Hellbardt, I. Behrmann, M. Germer, M. Pawlita, P.H. Krammer, and M.E. Peter. 1995. Cytotoxicity-dependent APO-1 (Fas/CD95)-associated proteins form a death-inducing signaling complex (DISC) with the receptor. *EMBO J.* 14:5579–5588. https://doi.org/10.1002/j.1460-2075.1995.tb00245.x

Kobielak, A., and E. Fuchs. 2006. Links between alpha-catenin, NF-kappaB, and squamous cell carcinoma in skin. *Proc. Natl. Acad. Sci. USA.* 103:2322–2327. https://doi.org/10.1073/pnas.0510422103

Lu, M., S. Marsters, X. Ye, E. Luis, L. Gonzalez, and A. Ashkenazi. 2014. E-cadherin couples death receptors to the cytoskeleton to regulate apoptosis. *Mol. Cell.* 54:987–998. https://doi.org/10.1016/j.molcel.2014.04.029

McCrea, P.D., M.T. Maher, and C.J. Gottardi. 2015. Nuclear signaling from cadherin adhesion complexes. *Curr. Top. Dev. Biol.* 112:129–196. https://doi.org/10.1016/bs.ctdb.2014.11.018

Niessen, C.M., D. Leckband, and A.S. Yap. 2011. Tissue organization by cadherin adhesion molecules: dynamic molecular and cellular mechanisms of morphogenetic regulation. *Physiol. Rev.* 91:691–731. https://doi.org/10.1152/physrev.00004.2010

Peter, M.E., R.C. Budd, J. Desbarats, S.M. Hedrick, A.O. Hueber, M.K. Newell, L.B. Owen, R.M. Pope, J. Tschopp, H. Wajant, et al. 2007. The CD95 receptor: apoptosis revisited. *Cell.* 129:447–450. https://doi.org/10.1016/j.cell.2007.04.031

Qian, X., T. Karpova, A.M. Sheppard, J. McNally, and D.R. Lowy. 2004. E-cadherin-mediated adhesion inhibits ligand-dependent activation of diverse receptor tyrosine kinases. *EMBO J.* 23:1739–1784. https://doi.org/10.1038/sj.emboj.7600136

Qin, Y., C. Capaldo, B.M. Gumbiner, and I.G. Macara. 2005. The mammalian Scribble polarity protein regulates epithelial cell adhesion and migration through E-cadherin. *J. Cell Biol.* 171:1061–1071. https://doi.org/10.1083/jcb.200506094

Ramaswamy, M., S.Y. Cleland, A.C. Cruz, and R.M. Siegel. 2009. Many checkpoints on the road to cell death: regulation of Fas-FasL interactions and Fas signaling in peripheral immune responses. *Results Probl. Cell Differ.* 49:17–47. https://doi.org/10.1007/400_2008_24

Reuver, S.M., and C.C. Garner. 1998. E-cadherin mediated cell adhesion recruits SAP97 into the cortical cytoskeleton. *J. Cell Sci.* 111:1071–1080.

Round, J.L., T. Tomassian, M. Zhang, V. Patel, S.P. Schoenberger, and M.C. Miceli. 2005. Dlgh1 coordinates actin polymerization, synaptic T cell receptor and lipid raft aggregation, and effector function in T cells. *J. Exp. Med.* 201:419–430. https://doi.org/10.1084/jem.20041428

Schindelin, J., I. Arganda-Carreras, E. Frise, V. Kaynig, M. Longair, T. Pietzsch, S. Preibisch, C. Rueden, S. Saalfeld, B. Schmid, et al. 2012. Fiji: an open-source platform for biological-image analysis. *Nat. Methods.* 9:676–682. https://doi.org/10.1038/nmeth.2019

Schneider, M.R., M. Dahlhoff, D. Horst, B. Hirschi, K. Trülzsch, J. Müller-Höcker, R. Vogelmann, M. Allgäuer, M. Gerhard, S. Steininger, et al. 2010. A key role for E-cadherin in intestinal homeostasis and Paneth cell maturation. *PLoS One.* 5:e14325. https://doi.org/10.1371/journal.pone.0014325

Stairs, D.B., L.J. Bayne, B. Rhoades, M.E. Vega, T.J. Waldron, J. Kalabis, A. Klein-Szanto, J.S. Lee, J.P. Katz, J.A. Diehl, et al. 2011. Deletion of p120-catenin results in a tumor microenvironment with inflammation and cancer that establishes it as a tumor suppressor gene. *Cancer Cell.* 19:470–483. https://doi.org/10.1016/j.ccr.2011.02.007

Stupack, D.G., and D.A. Cheresh. 2002. Get a ligand, get a life: integrins, signaling and cell survival. *J. Cell Sci.* 115:3729–3738. https://doi.org/10.1242/jcs.00071

Takeichi, M. 1988. The cadherins: cell-cell adhesion molecules controlling animal morphogenesis. *Development*. 102:639–655.

Theisen, C.S., J.K. Wahl III, K.R. Johnson, and M.J. Wheelock. 2007. NHERF links the N-cadherin/catenin complex to the platelet-derived growth factor receptor to modulate the actin cytoskeleton and regulate cell motility. *Mol. Biol. Cell.* 18:1220–1232. https://doi.org/10.1091/mbc.e06-10-0960

Vasioukhin, V., C. Bauer, L. Degenstein, B. Wise, and E. Fuchs. 2001. Hyperproliferation and defects in epithelial polarity upon conditional ablation of alpha-catenin in skin. *Cell.* 104:605–617. https://doi.org/10.1016/S0092-8674(01)00246-X

Weaver, V.M., S. Lelièvre, J.N. Lakins, M.A. Chrenek, J.C. Jones, F. Giancotti, Z. Werb, and M.J. Bissell. 2002. beta4 integrin-dependent formation of polarized three-dimensional architecture confers resistance to apoptosis in normal and malignant mammary epithelium. *Cancer Cell.* 2:205–216. https://doi.org/10.1016/S1535-6108(02)00125-3

Yanagisawa, J., M. Takahashi, H. Kanki, H. Yano-Yanagisawa, T. Tazunoki, E. Sawa, T. Nishitoba, M. Kamishohara, E. Kobayashi, S. Kataoka, and T. Sato. 1997. The molecular interaction of Fas and FAP-1. A tripeptide blocker of human Fas interaction with FAP-1 promotes Fas-induced apoptosis. *J. Biol. Chem.* 272:8539–8545. https://doi.org/10.1074/jbc.272.13.8539